Food Chemistry 230 (2017) 673–680

Contents lists available at ScienceDirect

Food Chemistry

journal homepage: www.elsevier.com/locate/foodchem

Analytical Methods

Highly sensitive fluorescence sensing of zearalenone using a novel aptasensor based on upconverting nanoparticles

Zhengzong Wu [a,b], Enbo Xu [a], Muhammad F.J. Chughtai [b,c], Zhengyu Jin [a,*], Joseph Irudayaraj [b,*]

[a] The State Key Laboratory of Food Science and Technology, School of Food Science and Technology, Jiangnan University, 1800 Lihu Road, Wuxi 214122, China
[b] Department of Agriculture & Biological Engineering, Bindley Bioscience Center, Purdue Center for Cancer Research, Purdue University, West Lafayette, IN 47907, USA
[c] National Institute of Food Science & Technology, University of Agriculture, Faisalabad, Pakistan

ARTICLE INFO

Article history:
Received 27 September 2016
Received in revised form 8 March 2017
Accepted 17 March 2017
Available online 19 March 2017

Keywords:
Biosensor
Zearalenone
Mycotoxin
Fluorescence
Magnetic nanoparticles

ABSTRACT

A facile strategy was successfully developed for the detection of zearalenone (ZEN). In this assay, highly fluorescent upconversion nanoparticles were synthesized and conjugated with the complementary oligonucleotide of ZEN aptamer for use as signal probes. Magnetic nanoparticles immobilized with the ZEN aptamer were assigned as capture probes. The results exhibited that the linear correlation between the decreased luminescence intensity of the signal and the concentration of ZEN was very strong (R^2 = 0.9957) in the range of 0.05–100 μg/L. In addition, the limit of detection of the proposed method (0.126 μg/kg for corn and 0.007 μg/L for beer) was significantly lower than the existing methods. Furthermore, the reliability of the competitive immunoassay format was validated by comparing the results determined in real food samples to those obtained from a commercially available method. Overall, the novel aptasensor have showed great potential for rapid and accurate ZEN determination.

1. Introduction

Zearalenone (ZEN), also known as F-2 toxin, is a nonsteroidal estrogenic mycotoxin biosynthesized through a polyketide pathway by several Fusarium species with widespread occurrence in corn, wheat, oat, barley, soybeans, beer, etc. (Liu et al., 2014). There is evidence that the consumption of ZEN contaminated products might cause various toxic effects on humans and animals (pigs, cattle and sheep), including teratogenesis, carcinogenicity, neurotoxicity, abortion, and estrogenic effect (Schneider & Dickert, 1994). It has been classified as a group III carcinogen by the International Agency for Research on Cancer (Zhang, Eremin et al., 2017). In order to limit the exposure to ZEN contaminated products, the tolerable levels of ZEN for different kinds of agricultural products have been established by many countries and organizations, including China (60 μg/kg for wheat, wheat flour, corn and corn flour and 500 μg/L for feed samples) (Zhan, Huang, Chen, Li, & Xiong, 2016), Japan (1000 μg/kg for compound feeds), Australia (50 μg/kg for cereal products) (Zinedine, Soriano, Molto, & Manes, 2007) and European Union (EU) (100 μg/kg for cereals and 350 μg/kg for unprocessed maize) (Zhang, Eremin et al., 2017; Zhang, Pan et al., 2017; Zhang, Tao, Niu, Li, & Chen, 2017).

Assured conformance with abovementioned standards demands the continuous monitoring of trace level of ZEN in agricultural commodities, cereal products, etc. Various methods have been employed for ZEN contents determination in foods or feedstuffs, including high-performance liquid chromatography (HPLC) (Ok, Choi, Kim, & Chun, 2014), liquid chromatography-mass spectrometry (LC-MS) (Soleimany, Jinap, Faridah, & Khatib, 2012), high performance thin layer chromatography (HPTLC) (Dawlatana, Coker, Nagler, Blunden, & Oliver, 1998; Hadiani, Yazdanpanah, Ghazi-Khansari, Cheraghali, & Goodarzi, 2003), electrochemical immunoassay (ECI) (Hervás, López, & Escarpa, 2009), fluorescence polarization immunoassay (FPI) (Chun, Choi, Chang, Choi, & Eremin, 2009), surface-enhanced Raman scattering immunoassay (SERSI) (Liu et al., 2014) and enzyme-linked immunosorbent assay (ELISA) (Kuzdraliński, Solarska, & Muszyńska, 2013; Zhang, Tao, Niu, Li, & Chen, 2017). Out of these sophisticated techniques, chromatographic methods are highly selective and accurate. However, most of these methods are time-consuming, require harmful solvents and depend on professional technology, expensive instruments, and tedious sample pretreatment. In contrast, the immunoassay-based methods (ELISA and SERSI) offer rapid means of detection, but they are strongly dependent on the use of susceptible and expensive antibodies. As a result, immunoassays often fail to provide accurate quantitative results and their efficiencies are hindered by the complex and repetitive protocols (Zhao et al., 2015). Therefore, it is urgently necessary to develop an alternative

* Corresponding authors.
E-mail addresses: jinlab2008@yahoo.com (Z. Jin), josephi@purdue.edu (J. Irudayaraj).

http://dx.doi.org/10.1016/j.foodchem.2017.03.100
0308-8146/

rapid and sensitive approach for ZEN detection in agricultural commodities.

In recent years, nanoscience with multidisciplinary and interdisciplinary features has offered great potential for the development of new analytical tools and instruments for bioanalysis (Wu et al., 2015). Upconversion nanoparticles (UCNPs) doped with lanthanide have attracted a tremendous amount of attention. Due to their appealing photo-physical properties, such as low autofluorescence background, good photochemical stability, large Stokes shifts nonblinking and nonbleaching emission, tunable fluorescence wavelength, deep penetration into biological samples, and relatively low toxicity, UCNPs are regarded as more promising fluorophores compare to traditional fluorescent material and have been used in medical field (Tang et al., 2015; Wu et al., 2017). Recently, UCNPs have been successfully applied for the determination of a wide variety of targets, such as mycotoxins, antibiotics and bacteria (Hu et al., 2016; Pan, Zhao, & Chen, 2015; Sun, Li, Koidis, & Chen, 2016). To the best of our knowledge, no such research has been conducted to determine ZEN contents in food products using UCNPs.

Aptamers, featured with small size, ease of synthesis and labeling, lack of immunogenicity, low production cost, high stability and target binding affinity and specificity, have been considered as a good alternative to antibodies. Aptamers are single-stranded DNA or RNA molecules that form sequence-defined unique structural forms (Zhang et al., 2015). A series of aptamers-based biosensors (aptasensor) have been developed for detection of mycotoxins, such as ochratoxin A, fumonisin B1 and aflatoxin B1 (McKeague et al., 2010; Shim, Kim, Mun, & Kim, 2014). Recently, ZEN aptamer was selected and identified by Chen et al. (2013) for the first time. To date, however, there have been no studies to develop aptasensor for detecting ZEN.

Herein, we first reports a sensitive UCNPs and magnetic nanoparticles (MNPs)-based aptasensor for the quantitative detection of ZEN. The detailed fabrication procedures of the bioassay system for ZEN detection based on upconversion and magnetic nanoparticles is schematically shown in Fig. 1. The luminescence bioassay platform was fabricated by immobilizing aptamer and its hybridized complementary strand (cDNA) onto the surfaces of MNPs and UCNPs, respectively, and then the aptamer-MNPs and cDNA-UCNPs was mixed to form the duplex structure. With the addition of the target (i.e., ZEN), the ZEN aptamer dissociated from its complementary DNA and preferentially bounded to ZEN, resulting a decrease in the fluorescent intensity of the emission peak. The novel strategy developed here provide the potential to realize high-throughput screening of ZEN in food products.

2. Materials and methods

2.1. Chemical reagents

ZEN, α-zearalenol (α-ZEN) and β-zearalenol (β-ZEN) was obtained from Sigma-Aldrich (Saint Louis, MO). Zearalenone-4-glucoside (ZEN-G) and Zearalenone-4-sulfate (ZEN-S) were purchased from ADHOC INTERTEK Co., Ltd. (Beijing, China). The other five mycotoxin standards (Aflatoxin B1 (AFB1), aflatoxin B2 (AFB2), ochratoxin A (OTA), fumonisin B1 (FB1), fumonisin B2 (FB2)) used to evaluate for specificity were purchased from Aladdin Industrial Inc. (Shanghai, China). Ammonium fluoride (NH_4F), (3-aminopropyl) triethoxysilane (APTES) and 1,6-hexanediamine and octadecene (ODE) were got from J & K Chemical Technology Co., Ltd. (Beijing, China). Glutaraldehyde, tetraethyl orthosilicate (TEOS), Ytterbium(III) Chloride hexahydrate ($YbCl_3$), Yttrium chloride hexahydrate (YCl_3) and Erbium chloride hexahydrate ($ErCl_3$)

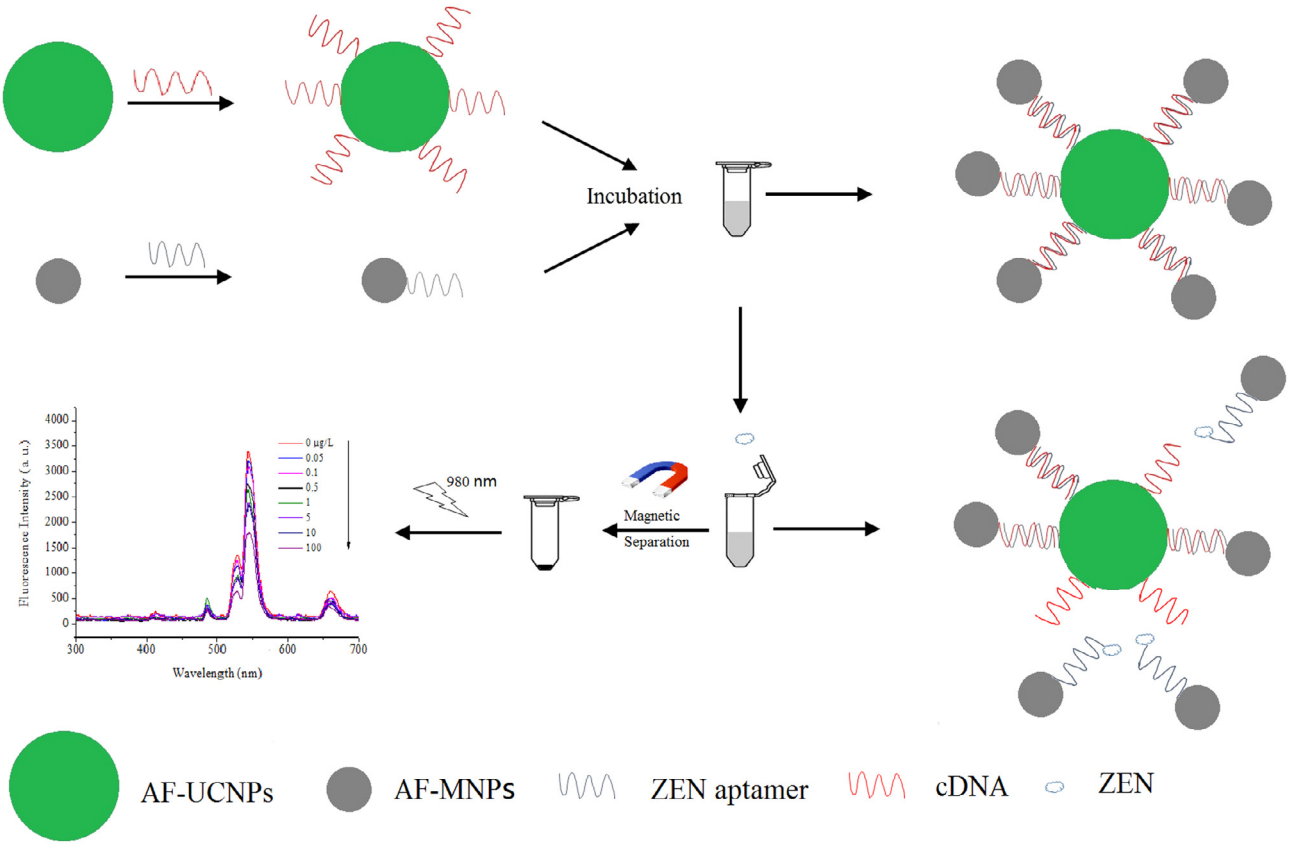

Fig. 1. Schematic illustration of the fabrication of the UCNPs-based aptasensor for the sensitive detection of ZEN.

were all purchased from Aladdin Industrial Inc. (Shanghai, China). Oleic acid (OA), iron chloride hexahydrate, Iron(II) chloride tetrahydrate, ethanol and methanol were obtained from Sinopharm Chemical Reagent Co., Ltd. (Shanghai, China). ZEN aptamer reported by Chen et al. (2013) and its complementary DNA fragments purified by HPLC were obtained from Aptagen, LLC (Jacobus, PA, USA).

2.2. Preparation and surface modification of nanoparticles

2.2.1. Synthesis of UCNPs

In this work, hexagonal $NaYF_4$: 18% Yb, 2% Er UCNPs were synthesized using a facile hydrothermal approach described by Li and Zhang (2008). Typically, 0.2427 g of YCl_3 (0.80 mmol), 0.0697 g of $YbCl_3$ (0.18 mmol) and 0.0076 g of $ErCl_3$ (0.02 mmol) were dissolved in 5 mL OA and 15 mL ODE in a 50 mL three-necked flask. The mixture was heated to 160 °C for 30 min to form a homogeneous yellow solution, and cooled down naturally to room temperature. Then 10 mL of methanol solution containing 0.1000 g NaOH and 0.1480 g NH_4F was slowly added to the flask, followed by stirring at 30 °C for 1 h to consume all fluoride. Subsequently, the solution was heated to 100 °C and maintained for 15 min, ensuring that the methanol was removed completely. Then the solution was heated up to 320 °C and kept for 1.5 h, with argon periodic purging. After cooling to room temperature, the nanocrystals were obtained by centrifugation at 5000 rpm. The precipitate from the solution was washed with ethanol-water (1:1 v/v) for several times. Finally, the obtained UCNPs were vacuum-dried at 60 °C overnight. OA-UCNPs were thus formed and kept in a desiccator for further use.

2.2.2. Surface modification of UCNPs

Surface modification of UCNPs was performed based on the method descripted by Stöber, Fink, and Bohn (1968) with few modifications. In brief, 2.5 ml UCNPs-cyclohexane dispersion (100 mg/mL) was added to a 250-mL flask, which contained 12.5 ml 25% ammonia and 100 mL ultrapure water. After the mixture had been vigorously stirred for 15 min, 300 μL TEOS was added for silica formation and keep stirring for 3 h. Then 500 μL APTES was added into the solution dropwise. The reaction was further maintained at room temperature for 1 h. After aging for 3 h, the obtained precipitates were centrifuged and washed with ethanol at least three times, and then dried in a vacuum oven for 12 h at 60 °C.

2.2.3. Preparation of MNPs

MNPs were prepared by a modified co-precipitation method (Chen et al., 2009; Zhang et al., 2017). $FeCl_3{\cdot}6H_2O$ (5.41 g) and $FeCl_2{\cdot}4H_2O$ (1.99 g) were dissolved in 100 mL of ultrapure water under N_2 in a 250 mL three-necked flask. After that, 30 mL of 5% ammonium hydroxide solution was added dropwise to the mixture at 80 °C under a nitrogen gas atmosphere After mechanical stirring for 30 min, the black precipitates obtained were collected from the reaction medium with the aid of an external magnet, and then washed with doubly distilled water several times to remove unreacted chemicals until the pH of the washings became close to neutral. Finally, the precipitate was dried at 60 °C in a vacuum oven and afterwards stored at 4 °C for further use.

2.2.4. Preparation of amine-functionalized MNPs

1 g MNPs synthesized above was added into 100 ml 0.4% APTES-ethanol solution and then the mixture was vigorously stirred for 6 h. The product was obtained by magnetic separation and repeated washing with ultrapure water and then dried under vacuum at 60 °C to obtain a black powder.

2.2.5. Aptamer or complementary DNA conjugation to nanoparticles

Before conjugation with oligonucleotides, the above amino-functionalized silica-modified UCNPs (AF-UCNPs) and amino-modified MNPs (AF-MNPs) were modified with streptavidin according to a classical glutaraldehyde method (Ye, Tan, Wang, & Yuan, 2004). Typically, 5 mL of 2 mg/mL AF-UCNPs or AF-MNPs phosphate buffered saline (PBS, 10 mM, pH 7.4) dispersions were mixed with 1.25 mL 25% glutaraldehyde, followed by shaking for 2 h at room temperature. Then, the MNPs were isolated using magnetic force while the UCNPs were separated by centrifugation. After washing with PBS for at least three times, the resultant nanoparticles were dispersed in 5 ml of 10 mM PBS again. Subsequently, the solution was mixed with 100 μL of 1.0 mg/mL streptavidin and shaken slowly on a shaking table for 12 h at room temperature. The avidin-conjugated nanoparticles were separated, washed with PBS, and dispersed in PBS again.

Based on the interaction between biotin and avidin, biotinylated zearalenone aptamer and its complementary DNA were connected on the surfaces of streptavidin-conjugated MNPs and UCNPs as follows: 240 μL of 1 μmol/L biotinylated zearalenone aptamer was mixed with 5 mL of the above avidin-conjugated MNPs dispersions and then the mixture was incubated for 12 h at 37 °C. To avoid the nonspecific absorption, excess aptamer was removed by centrifugation. Complementary DNA-linked UCNPs (cDNA-UCNPs) were fabricated following the same procedure. The prepared signal probe (cDNA-UCNPs) and capture probe (zearalenone aptamer-linked MNPs) were all resuspended in 10 mM PBS (pH 7.4) and stored at 4 °C for further use.

2.3. Characterization of nanoparticles

The size and morphology of nanoparticles were investigated by a high-resolution transmission electron microscope (TEM, JEM-2100, JEOL, Japan) equipped with a charge-coupled device (CCD) camera operating at an acceleration voltage of 200 kV as per the method reported by Tang et al. (2015). The TEM samples were prepared by dropping NPs solution onto copper grids coated with a thin carbon film and then it was allowed to dry under ambient condition. X-ray diffraction (XRD) measurements were performed to analyze the crystal structure of nanoparticles using an X-ray diffractometer (D2 PHASER, Bruker AXS Ltd., Germany) following the method reported by Hu, Sheng, Zhang, Wu, and Wang (2015). The surface groups of the bionanoparticles were identified by a FTIR spectrometer (Nicolet iS10, Thermo Electron Corp., Madison, WI, USA) in accordance with the procedure described by Sun et al. (2016). FTIR spectra was recorded in the range of 500-4000 cm^{-1} with 256 scans at a resolution of 4 cm^{-1}. The sample powders (5 mg) were ground with spectroscopic grade KBr powders (250 mg) and then pressed into 1 mm pellets. Upconversion fluorescence spectra were recorded on a Hitachi F-7000 fluorescence spectrophotometer (Hitachi Co., Tokyo, Japan) modified with an external 0–1300 mW adjustable continuous wave 980 nm laser (Beijing Hi-Tech Optoelectronic Co., Beijing, China) instead of the internal excitation source. UV–vis absorption spectra were collected using a commercial spectrometer TU-1900 (Purkinje General Corporation, Beijing, China) equipped with both deuterium and tungsten light source.

2.4. Immunoassay procedure

The procedure was partially referenced to the method reported by Pan et al. (2015) and Jin et al. (2017). An amount of 100 μL ZEN aptamer-linked MNPs and 600 μL of 0.1 mg/mL cDNA-UCNPs were first mixed in the Sodium Chloride-Tris-EDTA (STE) buffer (100 mM NaCl, 10 mM Tris-HCl, 1 mM EDTA, pH 8.0). Then the mixture was incubated at 37 °C for 1.5 h to form aptamer-linked

MNPs-cDNA UCNPs complex. The conjugates were purified by thorough washing, magnetic separation and dissolved in the PBS buffer. Thereafter, sample solutions containing various concentrations (0.05 μg/L, 0.1 μg/L, 0.5 μg/L, 1 μg/L, 5 μg/L, 10 μg/L and 100 μg/L) of ZEN standard were added to the above reaction system for incubation at 37 °C for 1 h. Then the remaining UCNPs-MNPs were isolated under magnetic force, washed several times and finally dispersed in PBS buffer again. The luminescence intensities in the absence (I_0) and in the presence (I) of ZEN were all recorded (543 nm was selected as the detection wavelength) and the difference (ΔI) between them were calculated for further use. For the blank (without ZEN), twenty measurements were performed. For other levels (0.05 μg/L, 0.1 μg/L, 0.5 μg/L, 1 μg/L, 5 μg/L, 10 μg/L and 100 μg/L), three measurements were performed.

2.5. Sample preparation and detection

Beer samples from Michelob Ultra brand were purchased from a local Walmart market (West Lafayette, IN, USA). This kind of beer is mainly made from wheat. The preparation of these samples was performed as follows. Each sample was stirred at 60 °C for approximately 60 min until complete degassing. After that, different ZEN concentrations (i.e., 5 μg/L, 10 μg/L and 50 μg/L) were added to the prepared samples for the contrast tests and standard addition and recovery experiments.

The ZEN-spiked corn samples were prepared according to the method reported by Liu et al. (2014) and Zhan et al. (2016) with some modifications. Different volumes of stock solutions (1 μg/mL and 10 μg/mL) were added to 5 g of pulverized corn samples to obtain corn samples spiked with different levels of ZEN (i.e., 90 μg/kg, 180 μg/kg and 900 μg/kg). The spiked samples were kept at room temperature for 3 h under to evaporate methanol in the corn samples. ZEN extraction was performed according to a previously reported method (Zhan et al., 2016) with some modifications. Specifically, 5 g of spiked sample was first mixed with 25 mL of methanol-water mixture (6:4, v/v) and 20 mL of 50 g/L NaCl solution, followed by shaking for 20 min. The mixture was centrifuged at 5000*g* for 10 min and then 3 mL of the supernatant solution was diluted with 3 mL of PBS and afterwards stored at 4 °C for further use. This solution was used to measure the ZEN contents with the developed aptasensor by the above-described procedure and validated by a commercially available ELISA method.

ELISA was performed according to the procedure suggested in the AgraQuant Zearalenone kit manual (Romer Laboratories, Union, MO). Briefly, standard solutions of ZEN or corn extracts were mixed with ZEN-horseradish peroxidase conjugate, and 100 μL of this mixture was incubated over the antibody solid phase for 10 min at room temperature. The 96-well microtiter plate was washed, and substrate was added to each well of the plate. Following incubation of the plate for 5 min at room temperature, the absorbance of each well was recorded using a microplate reader at 450 nm.

3. Results and discussions

3.1. Characterization

3.1.1. Characterization of UCNPs and MNPs

It was found that the structures of the synthesized OA-UCNPs and AF-UCNPs were hexagonal, which were consistent with standard XRD results of β-phase $NaYF_4$ crystals (JCPDS Standard Card No. 16-0334) (Fig. 2a). Furthermore, the XRD pattern of silica-coated UCNPs was similar to that of OA-UNCPs, indicating that the crystalline structure of UCNPs did not change during the surface modification process. It was worth noting that, owing to the coating approach, the diffraction intensities of AF-UCNPs were significantly lower than those of bare UCNPs. The reduced crystallinity of AF-UCNPs was calculated to be 15.57%.

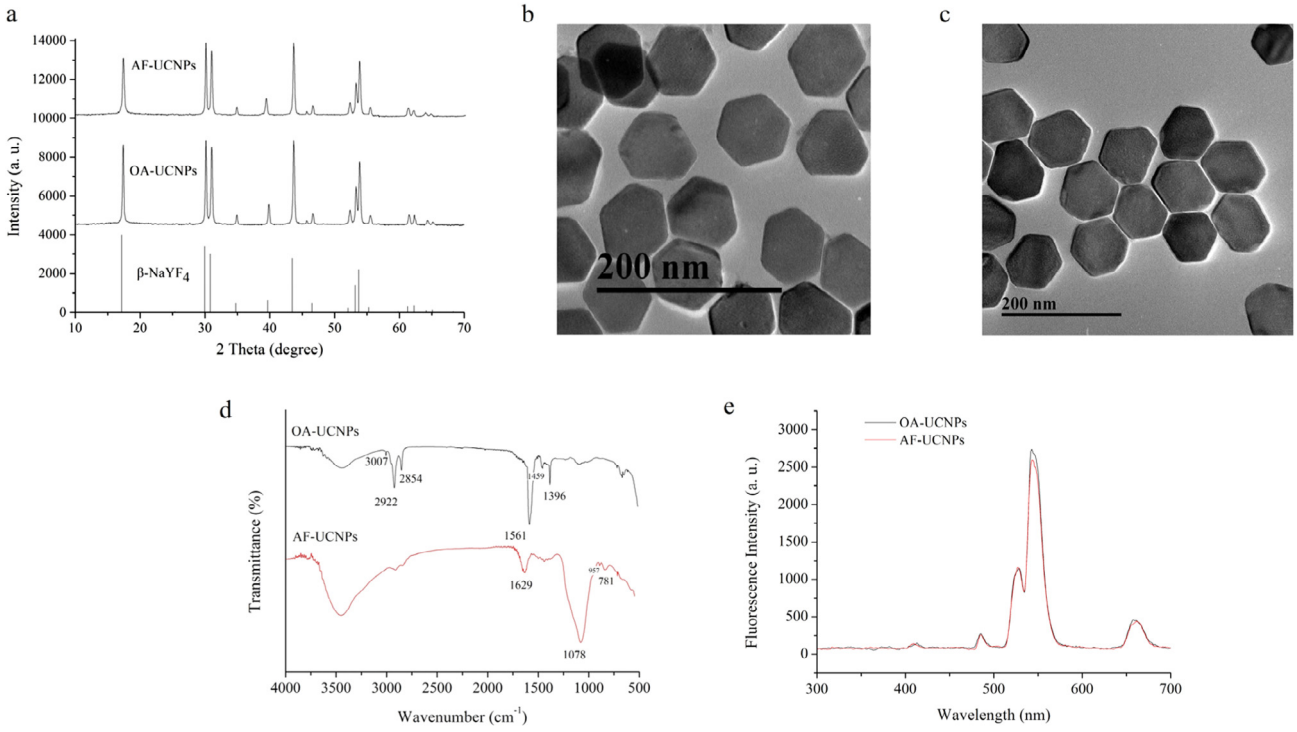

Fig. 2. (a) XRD patterns of AF-UCNPs and OA-UCNPs; (b) TEM image of OA-UCNPs; (c) TEM image of AF-UCNPs; (d) FTIR spectra of UCNPs before and after coating with silica shells; (e) fluorescence spectra of UCNPs with and without silica coating.

The formation of hexagonal nanostructured crystallites was further confirmed by the TEM images. Homogeneous and uniform nanoparticles before and after surface modification and bioconjugation were observed in Fig. 2 (both of Fig. 2b and c). The TEM images showed that the morphology of the UCNPs was characterized by well-dispersed and hexagonal nanocrystallines with a smooth surface. These nanoparticles had average uniform diameters of around 100 nm, which was in good accordance with the result calculated above. As could be seen in Fig. 2c, a thin silica shell was uniformly coated on the surface of the bare UCNPs.

The functional groups on the surfaces of OA-UCNPs and AF-UCNPs were identified by FTIR spectra. As shown in Fig. 2d, for both of OA-UCNPs and AF-UCNPs, a strong peak at approximately 3400 cm^{-1} corresponding to the stretching vibration of -OH compounds and hydroxide radicals was observed. This dominant absorption band was also observed by Hu et al. (2015). For OA-UCNPs, distinctive absorption bands were found at 1561 cm^{-1}, 1459 cm^{-1} and 1396 cm^{-1}, which was in consistence with that reported by Liu, Tan, and Yang (2013). These three bands were due to the stretching vibrations of carboxylic group ($-COO^-$) formed due to the interaction between the rare-earth ions and the carboxyl groups of OA molecules (Wu et al., 2015). In addition, the two peaks at 2922 and 2854 cm^{-1} could be assigned to the asymmetric and symmetric stretching vibrations of methylene group, respectively, which existed in the long alkyl chain of the oleic acid molecule. The positions of the two peaks were nearly the same to that reported by Wang et al. (2009). After surface modification of OA-UCNPs, the three characteristic absorption bands observed in the spectrum for OA-UCNPs disappeared. Compared with the spectrum of OA-UCNPs, two new peaks at 1078 cm^{-1}, the typical absorption peak of Si-O stretching vibration, and 1629 cm^{-1}, explained by the bending vibration from the amino group appeared in the spectrum of amino-modified UCNPs (Fang, Wu, Duan, Dai, & Wang, 2015) appeared in the spectrum for AF-UCNPs, which was in agreement with the results of Wang et al. (2009). At the same time, two small absorption peaks at approximately 957 cm^{-1} and 781 cm^{-1}, corresponding to the symmetric stretching vibrations of Si-O bond and the Si-O, respectively (Tian et al., 2015), were also observed in Fig. 1d. These observations suggested that the UCNPs had been successfully coated with a silica layer.

Fig. 2e showed the fluorescence spectra of OA-UCNPs and Amino-UCNPs excited with a 980 nm laser. It could be seen that, three dominant emission peaks at 407, 543 and 657 nm, respectively, were observed in the fluorescence spectra. These three peaks were mainly generated by the transitions from the $^2H_{9/2}$, $^4S_{3/2}$, and $^4F_{9/2}$ levels to the $^4I_{15/2}$ ground state of the Er^{3+} ion (Disney, Zheng, Swager, & Seeberger, 2004; Wang, Li, & Li, 2007).

The amino-modified MNPs were also characterized by TEM, XRD and FTIR. TEM images demonstrated that the synthesized MNPs were well-dispersed with an average size of approximately 10 nm (Fig. 3a). FTIR spectra were used to identify the functional groups existed in MNPs. As shown in Fig. 3b, a strong transmission band was observed at approximately 585 cm^{-1}, which was ascribed to the stretching vibration of the Fe-O bond from MNPs. In addition, absorption peaks associated with amino groups were

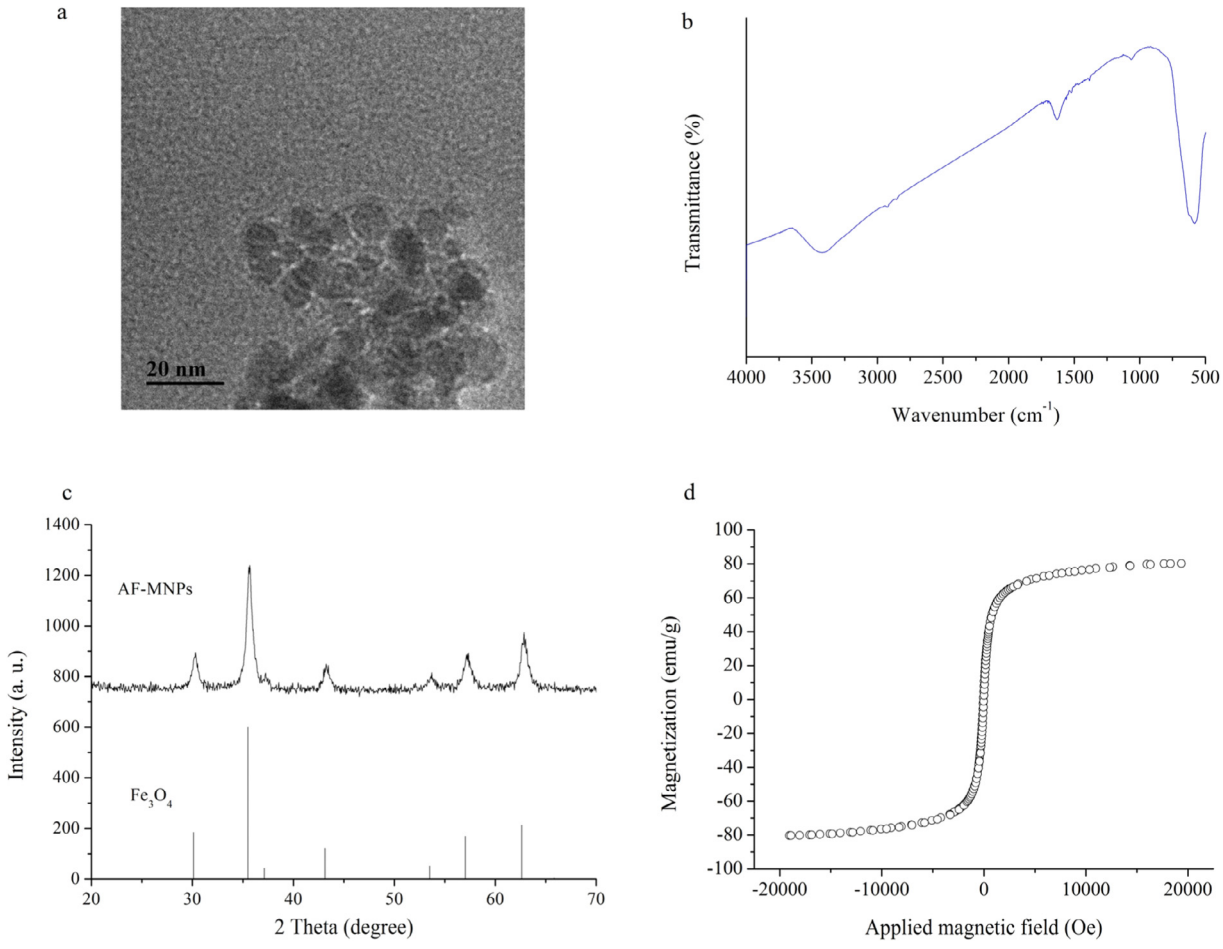

Fig. 3. (a) TEM image, (b) FTIR spectrum, (c) XRD pattern and (d) magnetization curve of AF-MNPs.

found at around 1631 cm^{-1} and 1056 cm^{-1}, revealing the existence of free -NH_2 groups on the amino-modified UCNPs. Furthermore, Six characteristic peaks for the MNPs were observed at 2θ = 30.20°, 35.66°, 43.14°, 53.37° and 62.76°. These peaks corresponded to (220), (311), (400), (422), (511) and (440) crystalline planes (Liu et al., 2016), respectively, which were in good accordance with the standard XRD diffraction patterns for Fe_3O_4 (JCPDS Standard Card No. 75-1610) (Fig. 3c). The sharp, strong peaks confirmed the products were well crystallized. MNPs with strong magnetic response play a key role for the magnetic separation and the accuracy of method. Thus, the magnetic property of the MNPs prepared in this study was also investigated by measuring the hysteresis loop at room temperature using vibrating sample magnetometer (VSM). The saturation magnetization of MNPs was determined to be as high as 80.25 emu/g (Fig. 3d), indicating that the MNPs synthesized in this study is intriguing in the separation approach.

3.1.2. Characterization of fluorescence signal probes and immunesensing probes

As shown in Fig. 4, for both of ZEN aptamer solution and cDNA solution, a strong absorption peak at 265 nm was observed in the UV–Vis spectra (Fig. 4a). After ZEN aptamer or cDNA had been incubated with the avidin-conjugated MNPs or amino-modified UCNPs, the supernatant was collected via magnetic separation or centrifugation. It was observed that the absorbance of the supernatant at 265 nm significantly decreased after the incubation (Fig. 4b). This is due to the fact that based on the interaction between biotin and avidin, biotinylated ZEN aptamer and its complementary DNA were connected on the surfaces of streptavidin-conjugated MNPs and UCNPs during the incubation process. At the end of the process, most of ZEN aptamer and its complementary DNA was conjugated with MNPs and UCNPs, respectively, which was similar to the results reported by Lv, Zhao, Wu, and Wang (2017). In addition, the effect of volume of ZEN aptamer solution on the conjugate ratio, which was defined as the ratio of the decreased absorbance of the supernatant solution to the solution of the original solution, was investigated in this study. As could be seen in Fig. 4a, the conjugate ratio kept nearly constant when the volume of ZEN aptamer solution increased from 180 μL to 240 μL, after which point, the conjugate ratio sharply decreased with the increase of the volume of ZEN aptamer solution. In consideration of both the conjugate efficiency and capacity, an optimal incubation volume of 240 μL was chosen in the present work.

Similarly, for the critical value that can make the surface of UCNPs conjugated with more cDNA, 210 μL cDNA solution was selected, as shown in Fig. 4b.

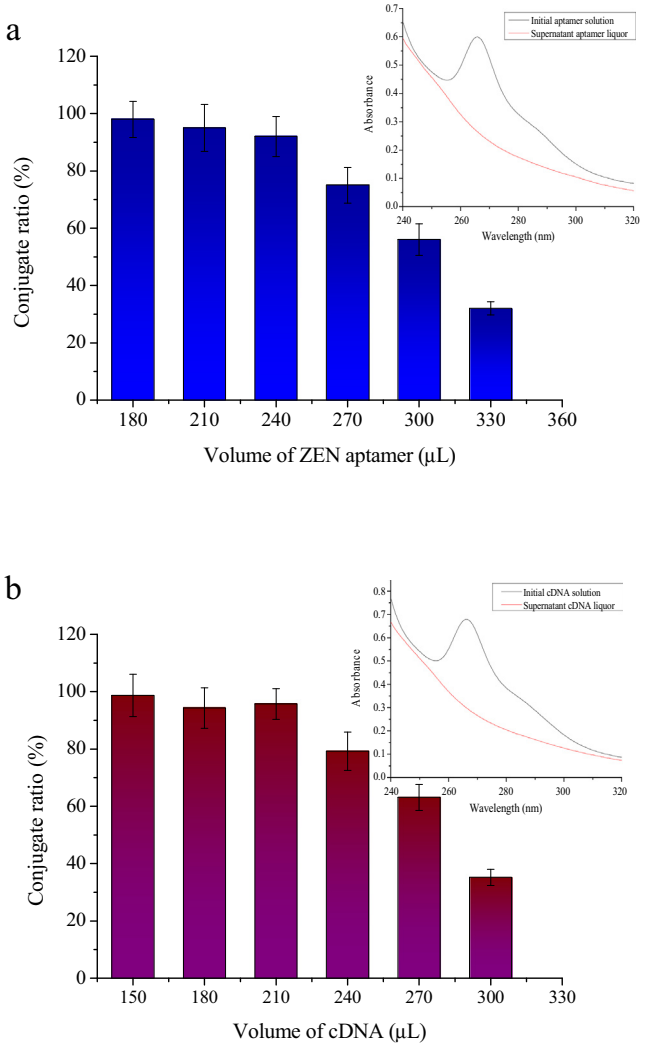

Fig. 4. (a) Optimization of the ZEN aptamer amount in capture probes (In set: UV–Vis absorption spectra of ZEN aptamer solution before and after conjugating with AF-MNPs); (b) Optimization of the cDNA amount in signal probes (Inset: UV–Vis absorption spectra of cDNA solution before and after conjugating with AF-UCNPs).

3.2. Optimization of the immunoassay

The optimal dosages of ZEN aptamer-MNPs was investigated in this study. For this, 100 μL ZEN aptamer-MNPs was mixed with various amounts of signal probes (100, 200, 300, 400, 500, 600, 700 and 800 μL). As shown in Fig. S1, the fluorescence signal gradually increased as the addition amount of signal probes increased. When the volume of the cDNA-UCNPs increased to 600 μL, the fluorescence intensity was the highest. Initially, only a small quantity of MNPs-UCNPs complex was formed on the basis of base pairing. When the concentration of ZEN aptamer-MNPs and the concentration of cDNA-UCNPs were matched (i.e., the capture probes reacted fully with the signal probes) the luminescence intensity reached a maximum. Therefore, 600 μL of signal probes was used in this work.

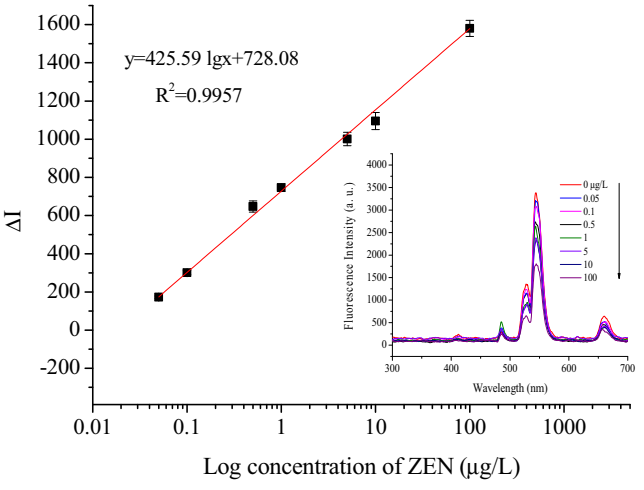

Fig. 5. Linear correlation between the decreased upconversion luminescent intensities and the concentrations of ZEN. The inset shows the typical recording output for detecting various ZEN concentrations using the proposed fluorescence immunoassay protocol.

Table 1
Detection and recovery results of ZEN in real samples by ELISA and the proposed method.

Sample	Background content (μg/L or μg/kg)	Spiked levels (μg/L or μg/kg)	Detected content (μg/L or μg/kg) (mean ± SD[a])		
			ELISA	This method	Recovery ratio (%)
Corn	28.62	90	110.52 ± 10.26	114.84 ± 6.31	96.81
	28.62	180	213.30 ± 13.85	202.32 ± 9.18	96.98
	28.62	900	860.76 ± 47.16	873.36 ± 48.64	94.05
	120.96	90	212.04 ± 17.82	213.66 ± 16.23	101.28
	120.96	180	296.82 ± 24.80	283.68 ± 18.97	94.26
	120.96	900	1018.31 ± 81.18	1064.78 ± 61.75	104.30
	680.94	90	755.28 ± 47.89	760.50 ± 60.12	98.65
	680.94	180	843.48 ± 61.74	875.88 ± 65.16	101.74
	680.94	900	1614.87 ± 94.68	1526.35 ± 141.3	96.54
Beer	4.82	5	9.74 ± 0.71	9.67 ± 0.72	98.47
	4.82	10	13.53 ± 0.84	13.84 ± 0.94	93.39
	4.82	50	55.83 ± 3.52	57.85 ± 4.17	105.53
	18.36	5	23.16 ± 2.07	24.08 ± 1.16	103.08
	18.36	10	28.28 ± 1.95	31.10 ± 1.38	109.66
	18.36	50	68.47 ± 4.69	67.23 ± 3.46	98.35
	48.65	5	52.88 ± 3.03	53.46 ± 3.02	99.65
	48.65	10	55.43 ± 6.10	56.82 ± 5.99	96.88
	48.65	50	99.18 ± 9.75	98.97 ± 10.87	100.32

[a] Standard deviation.

3.3. Analytical performance

Various intensities of the luminescence spectra obtained in the presence of different concentrations of ZEN was shown in Fig. 5. As could be seen in the figure, the changes of the fluorescent intensities gradually increased with the increase of the addition amount of the target molecules (ZEN). A good linearity between the decreases in the fluorescence intensities (ΔI) and the logarithm concentrations of ZEN was observed from 0.05 μg/L to 100 μg/L with a correlation coefficient of 0.9957 and a linear regression equation of y = 425.59 lgx + 728.08.

In this work, the detection limit (LOD) of the sensing system was 0.007 μg/L for beer and 0.126 μg/kg for corn, respectively. For comparison, the analytical performances of several conventional fluorescence-based detection methods for ZEN reported in the literature were listed in Table S1. As could be seen, compared with the current existing methods, the LOD obtained from the proposed method was much lower.

Chen et al. (2013) also developed a ZEN detection method based on a magnetic separation/preconcentration procedure using the ZEN aptamer. The working range (0.05–100 μg/L) of our method was broader than that of their assay. In addition, LOD (0.007 μg/L) of our method was much lower than that of their method (0.25 μg/L). Furthermore, in comparison with their method, our assay was more suitable to be applied in complex systems due to the unique advantages of UCNPs used in our method (FAM was used in their assay).

3.4. Evaluation of specificity

The selectivity and specificity of the proposed sensing method toward EC was evaluated by determining and comparing the fluorescent-signal changes caused by ZEN and its structure analogues (α-ZEN, β-ZEN, ZEN-G and ZEN-S) and five other mycotoxins (i.e. AFB 1, AFB 2, OTA, FB 1 and FB 2), which were widely-found in food raw materials. As illustrated in Fig. S2, among these targets, ZEN led to a dramatic fluorescence intensity change at 543 nm. Although the concentrations of the other targets (10 μg/L) were 10 times higher than ZEN (1 μg/L), the changes of the fluorescence intensities of them were still far below that observed for ZEN.

3.5. Analytical application

The accuracy of the proposed aptamer-based bioassay for determining ZEN levels in real food samples was evaluated by detecting ZEN in corn and beer samples spiked with a series of known quantities of ZEN. The results of recoveries were summarized in Table 1. All the three spiking levels applied showed good recoveries from 93% to 110%. In addition, food samples spiked with ZEN at three levels were analyzed by commercial ELISA kits to verify the practicability of the developed method. No significant difference ($p > 0.05$) between the results obtained by the applied bioanalysis method and those obtained using an ELISA method was observed, indicating that the proposed method has great potential for ZEN detection in corn and beer samples.

4. Conclusions

In summary, a novel biosensor for the determination of ZEN in food samples was established in this research. The biosensor combined the sensitivity of the upconverting nanoparticles (UCNPs), the specificity of the aptamer and the magnetic separation effect of MNPs. Excellent reorganization specificity, wide linear range and a low detection limit was achieved using this sensing system. In addition, the fabricated system was successfully applied for the fluorescence sensing of ZEN in corn and beer samples with good recoveries. These satisfactory results demonstrated that the novel fluorescent method developed on this work had great potential in the sensitive and economic detection of ZEN in food samples. This easy-to-operate method also could be extended to fluorescent detection for other mycotoxins, and this makes it a widely applicable approach for hazardous substances analysis.

Acknowledgements

This research was supported by funds from USDA-ARS (No. 1935-42000-049-00D) in conjunction with the Center for Food Safety Engineering at Purdue University, the Nature Science Foundation of Jiangsu Province (No. BK20160168), the Nature Science Foundation of China (Nos. 31601413 and 31501418) and the graduate student innovation project of Jiangsu Province (KYLX15_1134). The author Zhengzong Wu is thankful for the funding from Chinese Scholarship Council (CSC).

Appendix A. Supplementary data

Supplementary data associated with this article can be found, in the online version, at http://dx.doi.org/10.1016/j.foodchem.2017.03.100.

References

Chen, X., Huang, Y., Duan, N., Wu, S., Ma, X., Xia, Y., ... Wang, Z. (2013). Selection and identification of ssDNA aptamers recognizing zearalenone. *Analytical and Bioanalytical Chemistry, 405*(20), 6573–6581.

Chen, L., Liu, J., Zeng, Q., Wang, H., Yu, A., Zhang, H., & Ding, L. (2009). Preparation of magnetic molecularly imprinted polymer for the separation of tetracycline antibiotics from egg and tissue samples. *Journal of Chromatography A, 1216*(18), 3710–3719.

Chun, H. S., Choi, E. H., Chang, H.-J., Choi, S.-W., & Eremin, S. A. (2009). A fluorescence polarization immunoassay for the detection of zearalenone in corn. *Analytica Chimica Acta, 639*(1–2), 83–89.

Dawlatana, M., Coker, R., Nagler, M., Blunden, G., & Oliver, G. (1998). An HPTLC method for the quantitative determination of zearalenone in maize. *Chromatographia, 47*(3–4), 215–218.

Disney, M. D., Zheng, J., Swager, T. M., & Seeberger, P. H. (2004). Detection of bacteria with carbohydrate-functionalized fluorescent polymers. *Journal of the American Chemical Society, 126*(41), 13343–13346.

Fang, C., Wu, S., Duan, N., Dai, S., & Wang, Z. (2015). Highly sensitive aptasensor for oxytetracycline based on upconversion and magnetic nanoparticles. *Analytical Methods, 7*(6), 2585–2593.

Hadiani, M. R., Yazdanpanah, H., Ghazi-Khansari, M. M., Cheraghali, A., & Goodarzi, M. (2003). Survey of the natural occurrence of zearalenone in maize from northern Iran by thin-layer chromatography densitometry. *Food Additives & Contaminants, 20*(4), 380–385.

Hervás, M., López, M. Á., & Escarpa, A. (2009). Electrochemical immunoassay using magnetic beads for the determination of zearalenone in baby food: An anticipated analytical tool for food safety. *Analytica Chimica Acta, 653*(2), 167–172.

Hu, G., Sheng, W., Zhang, Y., Wang, J., Wu, X., & Wang, S. (2016). Upconversion nanoparticles and monodispersed magnetic polystyrene microsphere based fluorescence immunoassay for the detection of sulfaquinoxaline in animal-derived foods. *Journal of Agricultural and Food Chemistry, 64*, 3908–3915.

Hu, G., Sheng, W., Zhang, Y., Wu, X., & Wang, S. (2015). A novel and sensitive fluorescence immunoassay for the detection of fluoroquinolones in animal-derived foods using upconversion nanoparticles as labels. *Analytical and Bioanalytical Chemistry, 407*(28), 8487–8496.

Jin, B., Wang, S., Lin, M., Jin, Y., Zhang, S., Cui, X., ... Lu, T. J. (2017). Upconversion nanoparticles based FRET aptasensor for rapid and ultrasenstive bacteria detection. *Biosensors and Bioelectronics, 90*, 525–533.

Kuzdraliński, A., Solarska, E., & Muszyńska, M. (2013). Deoxynivalenol and zearalenone occurence in beers analysed by an enzyme-linked immunosorbent assay method. *Food Control, 29*(1), 22–24.

Li, Z., & Zhang, Y. (2008). An efficient and user-friendly method for the synthesis of hexagonal-phase NaYF 4:Yb, Er/Tm nanocrystals with controllable shape and upconversion fluorescence. *Nanotechnology, 19*(34), 345606.

Liu, J., Hu, Y., Zhu, G., Zhou, X., Jia, L., & Zhang, T. (2014). Highly sensitive detection of zearalenone in feed samples using competitive surface-enhanced Raman scattering immunoassay. *J Agric Food Chem, 62*(33), 8325–8332.

Liu, G., Li, T., Xin, Y., She, Y., Miao, W., Jing, W., ... Jin, M. (2016). Competitive fluorescence assay for specific recognition of atrazine by magnetic molecularly imprinted polymer based on Fe 3 O 4 -chitosan. *Carbohydrate Polymers, 137*, 75–81.

Liu, B., Tan, H., & Yang, C. (2013). Upconversion nanoparticle-based fluorescence resonance energy transfer assay for Cr(III) ions in urine. *Analytica Chimica Acta, 761*(2), 178–185.

Lv, J., Zhao, S., Wu, S., & Wang, Z. (2017). Upconversion nanoparticles grafted molybdenum disulfide nanosheets platform for microcystin-LR sensing. *Biosensors and Bioelectronics, 90*, 203–209.

McKeague, M., Bradley, C. R., Girolamo, A. D., Visconti, A., Miller, J. D., & DeRosa, M. C. (2010). Screening and initial binding assessment of fumonisin B1 aptamers. *International Journal of Molecular Sciences, 11*(12), 4864–4881.

Ok, H. E., Choi, S.-W., Kim, M., & Chun, H. S. (2014). HPLC and UPLC methods for the determination of zearalenone in noodles, cereal snacks and infant formula. *Food Chemistry, 163*, 252–257.

Pan, W., Zhao, J., & Chen, Q. (2015). Fabricating upconversion fluorescent probes for rapidly sensing foodborne pathogens. *Journal of Agricultural and Food Chemistry, 63*(36), 8068–8074.

Schneider, E. P., & Dickert, K. J. (1994). Health costs and benefits of fungicide use in agriculture: A literature review. *Journal of Agromedicine, 1*(1), 19–37.

Shim, W.-B., Kim, M. J., Mun, H., & Kim, M.-G. (2014). An aptamer-based dipstick assay for the rapid and simple detection of aflatoxin B1. *Biosensors and Bioelectronics, 62*, 288–294.

Soleimany, F., Jinap, S., Faridah, A., & Khatib, A. (2012). A UPLC–MS/MS for simultaneous determination of aflatoxins, ochratoxin A, zearalenone, DON, fumonisins, T-2 toxin and HT-2 toxin, in cereals. *Food Control, 25*(2), 647–653.

Stöber, W., Fink, A., & Bohn, E. (1968). Controlled growth of monodisperse silica spheres in the micron size range. *Journal of Colloid and Interface Science, 26*(1), 62–69.

Sun, C., Li, H., Koidis, A., & Chen, Q. (2016). Quantifying Aflatoxin B 1 in peanut oil using fabricating fluorescence probes based on upconversion nanoparticles. *Spectrochimica Acta Part A: Molecular and Biomolecular Spectroscopy, 165*, 120–126.

Tang, Y., Gao, Z., Wang, S., Gao, X., Gao, J., Ma, Y., ... Li, J. (2015). Upconversion particles coated with molecularly imprinted polymers as fluorescence probe for detection of clenbuterol. *Biosensors and Bioelectronics, 71*, 44–50.

Tian, J., Bai, J., Peng, Y., Qie, Z., Zhao, Y., Ning, B., ... Gao, Z. (2015). A core-shell-structured molecularly imprinted polymer on upconverting nanoparticles for selective and sensitive fluorescence sensing of sulfamethazine. *Analyst, 140*(15), 5301–5307.

Wang, L., Li, P., & Li, Y. (2007). Down- and up-conversion luminescent nanorods. *Advanced Materials, 19*(20), 3304–3307.

Wang, M., Mi, C.-C., Wang, W.-X., Liu, C.-H., Wu, Y.-F., Xu, Z.-R., ... Xu, S.-K. (2009). Immunolabeling and NIR-excited fluorescent imaging of HeLa cells by using NaYF4: Yb, Er upconversion nanoparticles. *ACS Nano, 3*(6), 1580–1586.

Wu, Z., Xu, E., Li, J., Long, J., Jiao, A., Jin, Z., & Xu, X. (2017). Determination of antioxidant capacity of Chinese rice wine and Zhuyeqing liquor using nanoparticle-based colorimetric methods. *Food Analytical Methods, 10*(3), 788–798.

Wu, Z., Xu, E., Long, J., Zhang, Y., Wang, F., Xu, X., ... Jiao, A. (2015a). Monitoring of fermentation process parameters of Chinese rice wine using attenuated total reflectance mid-infrared spectroscopy. *Food Control, 50*, 405–412.

Wu, S., Zhang, H., Shi, Z., Duan, N., Fang, C. C., Dai, S., & Wang, Z. (2015b). Aptamer-based fluorescence biosensor for chloramphenicol determination using upconversion nanoparticles. *Food Control, 50*, 597–604.

Ye, Z., Tan, M., Wang, G., & Yuan, J. (2004). Preparation, characterization, and time-resolved fluorometric application of silica-coated terbium(III) fluorescent nanoparticles. *Analytical Chemistry, 76*(3), 513–518.

Zhan, S., Huang, X., Chen, R., Li, J., & Xiong, Y. (2016). Novel fluorescent ELISA for the sensitive detection of zearalenone based on H 2 O 2-sensitive quantum dots for signal transduction. *Talanta, 158*, 51–56.

Zhang, X., Eremin, S. A., Wen, K., Yu, X., Li, C., Ke, Y., Jiang, H., Shen, J., & Wang, Z. (2017). Fluorescence polarization immunoassay based on a new monoclonal antibody for the detection of the zearalenone class of mycotoxins in maize. *Journal of Agricultural and Food Chemistry*.

Zhang, H., Ma, X., Liu, Y., Duan, N., Wu, S., Wang, Z., & Xu, B. (2015). Gold nanoparticles enhanced SERS aptasensor for the simultaneous detection of Salmonella typhimurium and Staphylococcus aureus. *Biosensors and Bioelectronics, 74*, 872–877.

Zhang, B., Pan, Y., Chen, H., Liu, T., Tao, H., & Tian, Y. (2017). Stabilization of starch-based microgel-lysozyme complexes using a layer-by-layer assembly technique. *Food Chemistry, 214*, 213–217.

Zhang, B., Tao, H., Niu, X., Li, S., & Chen, H.-Q. (2017). Lysozyme distribution, structural identification, and in vitro release of starch-based microgel-lysozyme complexes. *Food Chemistry, 227*, 137–141.

Zhao, Y., Yang, Y., Luo, Y., Yang, X., Li, M., & Song, Q. (2015). Double detection of mycotoxins based on SERS labels embedded Ag@ Au core-shell nanoparticles. *ACS Applied Materials & Interfaces, 7*(39), 21780–21786.

Zinedine, A., Soriano, J. M., Molto, J. C., & Manes, J. (2007). Review on the toxicity, occurrence, metabolism, detoxification, regulations and intake of zearalenone: An oestrogenic mycotoxin. *Food and Chemical Toxicology, 45*(1), 1–18.